Peptides 31 (2010) 1434–1440

Contents lists available at ScienceDirect

Peptides

journal homepage: www.elsevier.com/locate/peptides

Isolation and characterization of cytotoxic cyclotides from *Viola tricolor*

Jun Tang[a,c], Conan K. Wang[b], Xulin Pan[a], He Yan[a,c], Guangzhi Zeng[a], Wenyan Xu[a,c], Wenjun He[a,c], Norelle L. Daly[b], David J. Craik[b,**], Ninghua Tan[a,*]

[a] *State Key Laboratory of Phytochemistry and Plant Resources in West China, Kunming Institute of Botany, Chinese Academy of Sciences, 132# Lanhei Road, Heilongtan, Kunming 650204, Yunnan, PR China*
[b] *Institute for Molecular Bioscience, The University of Queensland, Brisbane, QLD 4072, Australia*
[c] *Graduate School of the Chinese Academy of Sciences, Beijing 100049, PR China*

ARTICLE INFO

Article history:
Received 29 March 2010
Received in revised form 10 May 2010
Accepted 10 May 2010
Available online 16 May 2010

Keywords:
Cyclotides
Viola tricolor
Cytotoxic activity
vitri B–F
varv Hm
varv He

ABSTRACT

Many plants of the Violaceae plant family have been used in traditional remedies, and these plants often contain cyclotides, a particular type of plant cyclopeptide that is distinguished by a cyclic cystine knot motif. In general, bioactive plant cyclopeptides are interesting candidates for drug development. In the current study, a suite of 14 cyclotides, which includes seven novel cyclotides [vitri B, C, D, E, F, varv Hm, and He], together with seven known cyclotides [varv A, D, E, F, H, vitri A, and cycloviolacin O2], was isolated from *Viola tricolor*, a common flower. A chromatography-based method was used to isolate the cyclotides, which were characterized using tandem mass spectrometry and NMR spectroscopy. Several of the cyclotides showed cytotoxic activities against five cancer cell lines, U251, MDA-MB-231, A549, DU145, and BEL-7402. Three cyclotides, vitri A, vitri F, and cycloviolacin O2, were the most cytotoxic. The cytotoxic activity of the cyclotides did not correlate well with their hemolytic activity, indicating that different interactions, most likely with membranes, are involved for cytotoxic and hemolytic activities. Homology modeling of the structures was used in deriving structure–activity relationships.

1. Introduction

Plant cyclopeptides are a diverse group of molecules, comprising eight structural types, including some of potential pharmaceutical interest [47]. Cyclotides, the group of pharmaceutically active plant cyclopeptides that are the focus of this study, are disulfide-rich macrocyclic proteins comprising 28–37 amino acid residues and well-defined three-dimensional structures [39]. Apart from a macrocyclic backbone, cyclotides are characterized by a cystine knot motif residing at their protein core, which is formed from six absolutely conserved Cys residues. The residues between successive Cys residues form backbone loops that project from this conserved core and presumably contribute to the observed bioactivities of cyclotides. The combination of a cyclic backbone and a cystine knot is termed the cyclic cystine knot (CCK) motif and this motif underpins the remarkable stability and pharmaceutical potential of cyclotides [13]. The key structural features of cyclotides are shown in Fig. 1 for kalata B1 (kB1) [38], the first characterized member of the cyclotide family, as an example. In early studies of cyclotides, isolation methods guided by mass spectrometry or bioassay were established [4,19]. More recently, molecular biological methods also have been used to explore the diversity of cyclotide sequences and to discover new cyclotide sequences [23,27,53]. So far, more than 150 cyclotides have been isolated from approximately 30 plants in the Violaceae and Rubiaceae families [50], and are divided into two major subfamilies, Möbius and bracelet, depending on the presence or absence, respectively, of a *cis*-Pro peptide bond in loop 5 [10]. Cyclotides have a range of interesting bioactivities, including uterotonic, anti-HIV, anti-fungal, cytotoxic, anti-bacterial, nematocidal, molluscicidal, hemolytic, neurotensin antagonistic, insecticidal, and trypsin inhibitory activities [6,12,14,37].

Viola tricolor L., a common horticultural plant, is a member of the Violaceae plant family, has been used in traditional medicine for heat-clearing, detoxification, and relieving coughs [43]. Following up on the reported medicinal properties of *V. tricolor*, previous studies have mainly focused on the contribution of non-peptidic compounds [21,34,51], such as flavonoids, to the observed anti-inflammatory, anti-oxidant, and anti-bacterial activities of *V. tricolor* extracts. In one study on the cytotoxicity of *V. tricolor* extracts, three cyclotides were reported to have potent cytotoxic activities [45]. As cyclotide-containing plants often express a large mixture of cyclotides, it is of interest to study *V. tricolor* in more detail to identify new cyclotides with cytotoxic activities. In the

* Corresponding author. Tel.: +86 871 5223800; fax: +86 871 5223800.
** Corresponding author. Tel.: +61 7 3346 2109; fax: +61 7 3346 2029.
E-mail addresses: nhtan@mail.kib.ac.cn (N. Tan), d.craik@imb.uq.edu.au (D.J. Craik).

0196-9781/$ – see front matter © 2010 Elsevier Inc. All rights reserved.
doi:10.1016/j.peptides.2010.05.004

current study, 14 cyclotides from *V. tricolor* were isolated, and characterized by MS/MS and 2D NMR. The cyclotides were tested for cytotoxic and hemolytic activities, and were analyzed for their structure–activity relationships by homology modeling of cyclotide structures.

2. Materials and methods

2.1. General experimental procedures

Column chromatography was performed over macroporous resin (D 101, Tianjin Agrichemicals Co., China), polyamide (100–200 mesh, Taizhou Sijiashenhua Plastic Co., China), reverse phase C_{18} (40–63 μm, Merk, Germany), and Sephadex LH-20 (25–100 μm, Pharmacia Fine Chemicals Co., Sweden). Thin layer chromatography was performed on silica gel plates (Qingdao Marine Chemicals Co., China). The improved Coomassie brilliant blue G-250 reagent was prepared as follows: 100 mg G-250 was dissolved in 20 mL ethanol, then added 20 mL phosphoric acid and 160 mL 50% ethanol. The ninhydrin reagent was a 0.2% ethanol solution [50]. HPLC was carried out on an Agilent 1100 series system with a UV detector at variable wavelengths of 206, 215, 225, 254, and 280 nm. Masses were analyzed on a Micromass LCT mass spectrometer equipped with an electrospray ionization source. For MALDI-TOF mass spectrometry (MS) analysis, the instrument was a Voyager DE-STR mass spectrometer (Applied Biosystems); 200 shots per spectra were acquired in positive ion reflector mode. The laser intensity was set to 2300, the accelerating voltage to 20,000 V, and the grid voltage to 64% of the accelerating voltage; the delay time was 165 ns. The low mass gate was set to 500 Da. Data were collected between 500 and 5000 Da. Calibration was undertaken using a peptide mixture obtained from Sigma–Aldrich (MSCal1). Nanospray MS/MS analysis was conducted on a QStar mass spectrometer; a capillary voltage of 900 V was applied, and the spectra were acquired at m/z 300–2000 for TOF spectra and m/z 60–2000 for product ion spectra. The collision energy for peptide fragmentation was varied between 10 and 50 V, depending on the size and charge of the ion. The analyst software program was used for data acquisition and processing.

2.2. Plant and cell materials

V. tricolor was grown at the Kunming Botanical Garden in Kunming as a seasonal ornamental, and was collected from the garden when it was out of season in April 2006. A voucher sample is held at the KUN herbarium, Kunming Institute of Botany, Chinese Academy of Sciences. Cancer cell lines, *i.e.* U251, MDA-MB-231, A549, DU145 and BEL-7402, were purchased from the Cell Culture Center of Institute of Basic Medical Science, Chinese Academy of Medical Sciences, Beijing, China.

2.3. Isolation and purification of cyclotides from V. tricolor

Dry whole herbs of *V. tricolor* (50 kg) were extracted by maceration for 24 h with 100% ethanol twice at room temperature, followed by extraction with ethanol/water (1:1, v/v) three times [47,52]. After the combined organic extracts were concentrated to 20 L (without ethanol), the liquid extract was partitioned, in turn, between H_2O and petroleum ether, H_2O and ethyl acetate, H_2O and *n*-butanol (*n*-BuOH). The *n*-BuOH fraction was subjected to macroporous resin (D 101) column chromatography and eluted with increasing amounts of ethanol (*i.e.* 30% ethanol, 70% ethanol, and 95% ethanol). The cyclotide-containing fraction was separated by polyamide chromatography eluted with 20% ethanol, 50% ethanol and 80% ethanol, and by reverse phase C_{18} chromatography eluted with 40% ethanol, 70% ethanol and 95% ethanol, and finally by gel permeation on Sephadex LH-20 eluted with 70% ethanol. All the separating steps were detected by TLC plates with 0.2% ninhydrin ethanol solution and improved Coomassie brilliant blue G-250 solution to choose cyclotide-containing fractions for further isolation using the various column chromatography methods [52,54]. Final purification was achieved by HPLC on an Agilent 1100 series system with a UV detector at variable wavelengths of 206, 215, 225, 254, and 280 nm.

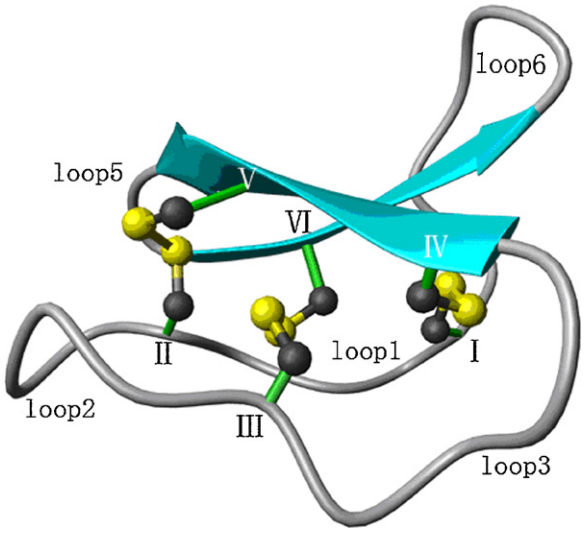

Fig. 1. Structure of kB1 (PDB ID: 1NB1). Cyclotides have a well-defined three-dimensional structure, stabilized by a cystine knot and a cyclic peptide backbone. Cyclotides have six loops and six Cys residues, labeled I–VI. β-Strands are indicated with darkened arrows.

2.4. Reduction of cyclotides and MALDI-MS analysis

To ca. 6 nmol of cyclotides in 20 μL of 0.1 M NH_4HCO_3 (pH 8.0), 1 μL of 0.1 mM tris(2-carboxyethyl) phosphine (TCEP) was added, and the solution was incubated at 55 °C for 30 min. The reduction was confirmed by MALDI-TOF MS after desalting using Ziptips (Millipore), which involved several washing steps followed by elution in 10 μL of 80% CH_3CN (0.5% HCO_2H). The desalted samples were mixed in a 1:1 ratio with matrix consisting of a saturated solution of α-cyano-4-hydroxcinnamic acid (CHCA) in 50% CH_3CN (0.5% HCO_2H).

2.5. Enzymatic digestion and nanospray MS/MS sequencing

To the reduced cyclotides, a combination of endoGluC and trypsin or a combination of endoGluC and chymotrypsin was added, to give a final cyclotide-to-enzyme ratio of 50:1 and the mixture was incubated at 37 °C for 3 h. The digestions were quenched by the addition of an equal volume of 0.5% HCO_2H and desalted using Ziptips (Millipore). Samples were stored at 4 °C prior to analysis. The fragments resulting from the digestions were first examined by MALDI-TOF MS followed by nanospray MS/MS analysis on a QStar mass spectrometer. MS/MS spectra were examined and used to sequence the cyclotides based on b- and y-series of ions present (N- and C-terminal fragments).

2.6. NMR sample analysis

Cyclotides were dissolved in 500 μL 90% H_2O/10% D_2O to a concentration of 1 mM at pH 3. Spectra were recorded on a Bruker Avance 500 or 600 MHz spectrometers at a sample temperature of 298 K. For resonance assignment a set of two-dimensional spectra, including TOCSY, with a mixing period of 80 ms, and NOESY with a

mixing time of 200 ms, were recorded. All two-dimensional spectra were collected over 4096 data points in the f2 dimension and 512 increments in the f1 dimension. Spectra were processed using TOPSIN (Bruker), and analyzed with Sparky 3.14. Chemical shifts were referenced to water at 4.75 ppm.

2.7. Homology modeling of cyclotides

The sequences of cyclotides were determined using mass spectrometry and two-dimensional NMR. Their structures were modeled on template structures, according to the results of searching the Protein Data Bank using the Build module of Modeller 9v5 [15]. The homology modeling of the cyclotides involved three main steps as follows.

2.7.1. Homology modeling

Template sequences were chosen from the Protein Data Bank (PDB) by searching for homologous sequences of the *V. tricolor* cyclotides in the PDB using the Composer package of Modeller 9v5. The structures of varv H, Hm, and He were aligned on kalata B2 (PDB ID: 1PT4); the structures of varv A, D, E, vitri B, C and E were aligned on kalata B1 (PDB ID: 1NB1); the structures of vitri A, vitri F, and cO2 were aligned on vhr1 (PDB ID: 1VB8); the structure of vitri D was aligned on varv F (PDB ID: 2K7G). The 3D structures of the cyclotides were built according to the alignment of sequences using the Build package of Modeller 9v5.

2.7.2. Optimizing for structural models

The 3D structures of cyclotides were selected according to the scores of Modeller and further optimized by Amber 10 using the FF03 force field. Hydrogen atoms were added by the xLEaP module of Amber10 and each system was solvated by adding a spherical TIP3P water grid of radius 12 Å. 2000 cycle minimizations were performed, including 1000 of steepest descent and 1000 of conjugate gradient energy minimizations based on 10.0 kcal/mol Å restraints. Similar energy minimizations were done except the restraints were set to 0.0 kcal/mol $Å^2$ [3].

2.7.3. Analysis for structures

Electrostatic potential and hydrophobicity surface of optimized structures of cyclotides were generated by the MolCAD package of Sybyl 7.3 [2].

2.8. Hemolytic assay

Cyclotides were dissolved in water and serially diluted in phosphate-buffered saline (PBS) to give 20 μL test solutions in a 96-well U-bottomed microtiter plate (Nunc). Human type O red blood cells (RBCs) were washed with PBS and centrifuged at 4000 rpm for 60 s in a microcentrifuge several times until a clear supernatant was obtained. A 0.25% suspension of washed RBCs in a PBS was added (1000 μL) to the cyclotides solutions. The plate was incubated at 37 °C for 1 h and centrifuged at 150 × *g* for 5 min. Aliquots of 100 μL were transferred to a 96-well flat-bottomed microtiter plate (Falcon), and the absorbance was measured at 415 nm with an automatic Multiskan Ascent Plate Reader (Labsystems). The level of hemolysis was calculated as the percentage of maximum lysis (1% Triton X-100 control) after adjusting for minimum lysis (PBS control). Synthetic melittin (Sigma) was used for comparison.

2.9. Cytotoxic assay

The sulforhodamine B (SRB) assay has been adopted for a quantitative measurement of cell growth and viability [20]. Cells were cultured in RPMI 1640 medium (Sigma). Aliquots of 90 μL were seeded in 96-well flat-bottomed microtiter plates (Greiner) with 3.3–7.7 × 10^4 cells/mL. Twenty-four hours later, 10 μL cyclotides, dissolved in DMSO and diluted with the medium, were added to the well with a final concentration of 10 μg/mL. After incubation at 37 °C and 5% CO_2 for another 48 h, cells were fixed by the addition of 50% ice-cold trichloroacetic acid and left at 4 °C for 1 h. After washing, air-drying, and staining for 15 min with 100 μL 0.4% SRB in 1% glacial acetic acid, excessive dye was removed by washing with 1% glacial acetic acid. After plates were air-dried, SRB was resuspended in 100 μL 10 mM Tris buffer, and the absorbance was measured at 560 nm with a Plate Reader (Molecular Devices, SPECTRA MAX 340). Cell growth inhibition was expressed as IC_{50} values (50% inhibitory concentration), which were calculated by dose–response curves with serial 5-fold cyclotides dilutions. Taxol, clinically used as an anti-cancer natural drug, was used as a positive control.

3. Results

3.1. Cyclotide isolation

To isolate cyclotides from *V. tricolor*, we modified a published approach that has been used to extract and isolate polypeptides from plants [4], and used the thin layer chromatography (TLC) detection method that we have developed specifically for cyclotide detection from crude plant extracts with improved Coomassie brilliant blue G-250 solution [52]. The extractions yielded 14 cyclotides.

3.2. Structural characterization

The cyclotides from *V. tricolor* were characterized by MS/MS and 2D NMR. One of the cyclotides exhibited a $[M+2H]^{2+}$ ion peak at *m/z* 1483.75^{2+} in the positive ESI MS, corresponding to a $[M+H]^+$ ion peak at *m/z* 2966.50^+. Reduction of this peptide with tris (2-carboxyethyl) phosphine (TCEP) resulted in an increase in molecular weight of 6 Da, consistent with the presence of three disulfide bonds. Treatment of the reduced peptide with trypsin/endoGluC produced two fragments of 2207 and 2990 Da. The 2990 Da fragment, 24 Da higher than the wild-type molecular weight, is consistent with the presence of three disulfide bonds and the addition of one H_2O, which suggests that the peptide is cyclic with three disulfide bonds. Treatment of the reduced peptide with chymotrypsin/endoGluC produced fragments of 1259, 1749, and 2990 Da. The 2207, 2990, 1259 and 1749 Da fragments were analyzed, and their sequences were elucidated as TCVGGTCNTPGCFCTWPVCTR, NGLPICGETCVGGTCNTPGCFCTWPVCTR, TCVGGTCNTPGCF, and CTWPVCTRNGLPICGE, respectively. Analysis of the TOCSY and NOESY spectra of the peptide indicated connectivities between spin systems consistent with the sequences VCTRNGL, ICGETCVGGTCNT, and GCFCT. The peptide sequence was determined by overlapping the aforementioned peptides from 2D NMR and MS/MS, and comparing these to published cyclotides documented within Cybase [50]. From these processes, the sequence was found to be cyclo-(GLPI^{I}CGET^{II}CVGGT^{III}CNTPG^{IV}CF^{V}CTWPV^{VI}CTRN), a new cyclotide named vitri C.

The other 13 cyclotides were characterized using a similar process to vitri C, and were confirmed as new cyclotides vitri B, D, E, F, varv Hm, He, and known cyclotides varv A, D, E, F, H, vitri A and cO2 [18,32,45], respectively. Their sequences, together with some molecular characteristics, are shown in Fig. 2. Based on the presence or absence of a putative *cis*-Pro residue in loop 5, the above cyclotides can be classified into two subfamilies, *i.e.* vitri B, C, D, E, varv Hm, He, H, A, D, E and F belonging to the Möbius subfamily, and vitri A, F and cO2 belonging to the bracelet subfamily. In addition to containing six absolutely conserved cysteine residues, both

cyclotides	structures	molecular weight (Da)	amino acid residues	molecular formula	charge
vitri B	GYPI^{5}CGES^{9}CVGGT^{14}CNTP—G^{19}CS^{21}CS–WPV^{26}CTTN	2872	29	$C_{117}H_{171}N_{32}O_{41}S_6$	-1
vitri C	GLPI^{5}CGET^{9}CVGGT^{14}CNTP—G^{19}CF^{21}CT–WPV^{26}CTRN	2965	29	$C_{124}H_{186}N_{36}O_{38}S_6$	0
vitri D	GLPV^{5}CGET^{9}CFTGS^{14}CYTP—G^{19}CS^{21}CN–WPV^{26}CNRN	3044	29	$C_{127}H_{183}N_{35}O_{40}S_6$	0
vitri E	GLPV^{5}CGET^{9}CVGGT^{14}CNTP—G^{19}CS^{21}CS–WPV^{26}CFRN	2923	29	$C_{121}H_{180}N_{34}O_{38}S_6$	0
vitri F	GTLP^{5}CGES^{9}CVWIP^{14}CISSVVG^{21}CA^{23}CK–SKV^{28}CYKD	3211	31	$C_{138}H_{216}N_{32}O_{41}S_6$	+1
varv Hm	GLPV^{5}CGET^{9}CFGGT^{14}CNTP—G^{19}CS^{21}CETWPV^{27}CSRN (Glu$_{22}$methylation)	3068	30	$C_{126}H_{187}N_{36}O_{42}S_6$	0
varv He	GLPV^{5}CGET^{9}CFGGT^{14}CNTP—G^{19}CS^{21}CETWPV^{27}CSRN (Glu$_{22}$ethylation)	3082	30	$C_{127}H_{189}N_{36}O_{42}S_6$	0
varv H	GLPV^{5}CGET^{9}CFGGT^{14}CNTP—G^{19}CS^{21}CETWPV^{27}CSRN	3054	30	$C_{125}H_{185}N_{36}O_{42}S_6$	-1
varv A	GLPV^{5}CGET^{9}CVGGT^{14}CNTP—G^{19}CS^{21}CS–WPV^{26}CTRN	2877	29	$C_{116}H_{178}N_{34}O_{39}S_6$	0
varv D	GLPI^{5}CGET^{9}CVGGS^{14}CNTP—G^{19}CS^{21}CS–WPV^{26}CTRN	2877	29	$C_{116}H_{178}N_{34}O_{39}S_6$	0
varv E	GLPI^{5}CGET^{9}CVGGT^{14}CNTP—G^{19}CS^{21}CS–WPV^{26}CTRN	2991	30	$C_{121}H_{186}N_{36}O_{41}S_6$	0
varv F	GVPI^{5}CGET^{9}CTLGT^{14}CYTA—G^{19}CS^{21}CS–WPV^{26}CTRN	2958	29	$C_{122}H_{189}N_{34}O_{40}S_6$	0
vitri A	G–IP^{4}CGES^{8}CVWIP^{13}CITSAIG^{20}CS^{22}CK–SKV^{27}CYRN	3154	30	$C_{134}H_{208}N_{37}O_{39}S_6$	+2
cO2	G–IP^{4}CGES^{8}CVWIP^{13}CISSAIG^{20}CS^{22}CK–SKV^{27}CYRN	3139	30	$C_{133}H_{208}N_{37}O_{39}S_6$	+2

Fig. 2. The primary structures and basic characteristics of cyclotides from *V. tricolor*. The first seven cyclotides in the list are novel and are reported for the first time here. The others are known cyclotides. Three of the cyclotides (vitri A, vitri F and cO2) are from the bracelet subfamily and the others are Möbius cyclotides.

the Möbius and bracelet subfamilies, have a consensus sequence of Gly-Glu-Thr/Ser in loop 1, and Ser/Thr in loop 4. The new peptides isolated in the current study conform to these consensus patterns, with the exception of vitri C and F which are the first two cyclotides to be found with a Phe and an Ala in loop 4, respectively.

3.3. Hemolytic activity

Nine of the isolated cyclotides were tested for hemolytic activity on human type O red blood cells (RBCs), and the results are shown in Fig. 3. The well-known hemolytic peptide melittin was used as a positive control. The results revealed that the cyclotides have varying levels of hemolytic activity, with HD_{50} values ranging from 4.29 to 225.90 μM. vitri B showed the least hemolysis, and vitri D was the most potent.

3.4. Cytotoxic activity

All cyclotides were tested for cancer cell toxicity against five human cancer cell lines: U251, MDA-MB-231, A549, DU145 and BEL-7402. We chose these cell lines in assays because they are from five different cancers. Table 1 summarizes the results, which revealed that several of the cyclotides are active against cancer cells. The most potent cyclotides, which are vitri A, F and cO2, which are all bracelet cyclotides and have IC_{50} values of 2.74–17.05 μg/mL against all tested cell lines. The IC_{50} values of the Möbius cyclotides against U 251 vary from 37.18 to 74.39 μg/mL.

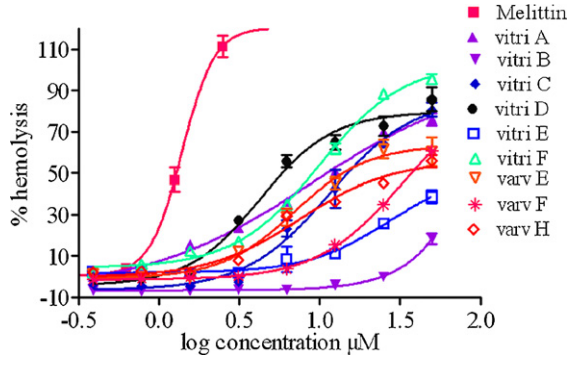

Fig. 3. Hemolytic activity of cyclotides from *V. tricolor*. Hemolytic activities of vitri A–F, varv E, F, H, and melittin were measured for human type O red blood cells. The HD_{50} values were calculated using Prism software to be 8.91 μM for vitri A, 225.90 μM for vitri B, 11.53 μM for vitri C, 4.29 μM for vitri D, 27.06 μM for vitri E, 10.00 μM for vitri F, 6.96 μM for varv E, 33.04 μM for varv F, 7.52 μM for varv H, and 0.93 μM for melittin. Melittin is a well-known hemolytic agent that was used as a positive control and gave an activity consistent with literature values.

3.5. Homology modeling of cyclotide structures

The structures of all cyclotides were built by Modeller 9v5, optimized by Amber 10, and analyzed by Sybyl 7.3 (Fig. 4). In comparison with other reported cyclotides, these cyclotides show characteristic clustering of hydrophobic and hydrophilic residues, but the distributions of these clusters show some differences. The highly hydrophobic patches on the molecular surfaces (brown areas) are formed by Val in loop 2, Trp and Pro in loop 5 in the Möbius cyclotides (vitri B, C, D, E, varv Hm, He, H, A, D, E and F), but by Val, Trp, Ile and Pro in loop 2 in the bracelet cyclotides (vitri A, F and cO2). Trp is at the center of the hydrophobic patches in both subfamilies. The distribution of the highly hydrophobic residues is concentrated for the bracelet cyclotides, but dispersed for the Möbius cyclotides.

4. Discussion

Plants often contain various types of components, which makes it difficult to guide isolating cyclotides from them. In this work, we adopted an improved Coomassie brilliant blue G-250 solution and 0.2% ninhydrin ethanol solution to guide cyclotide detection in the early stages of the isolation procedure to eliminate non-cyclotides, instead of a dependence on mass spectrometry or bio-assay as

Table 1
Cancer cell toxicity of cyclotides from *V. tricolor*.

Cyclotides	IC_{50} (μg/mL)				
	U251	MDA-MB-231	A549	DU145	BEL-7402
vitri B	45.21	>10	>10	>10	>10
vitri C	46.96	>10	>10	>10	>10
vitri D	51.65	>10	>10	>10	>10
vitri E	54.39	>10	>10	>10	>10
vitri F	6.31	2.74	3.58	3.44	5.36
varv Hm	74.39	>10	>10	>10	>10
varv He	55.43	>10	>10	>10	>10
varv H	44.70	>10	>10	>10	>10
varv A	37.18	>10	>10	>10	>10
varv D	46.62	>10	>10	>10	>10
varv E	38.84	>10	>10	>10	>10
varv F	44.49	>10	>10	>10	>10
vitri A	6.03	3.69	3.90	3.07	4.94
cO2	17.05	4.81	5.99	5.08	6.07
taxol	0.008	3.14[a]	0.02	0.05	0.058

[a] 10-Hydroxycamptothecin was used as the positive control.

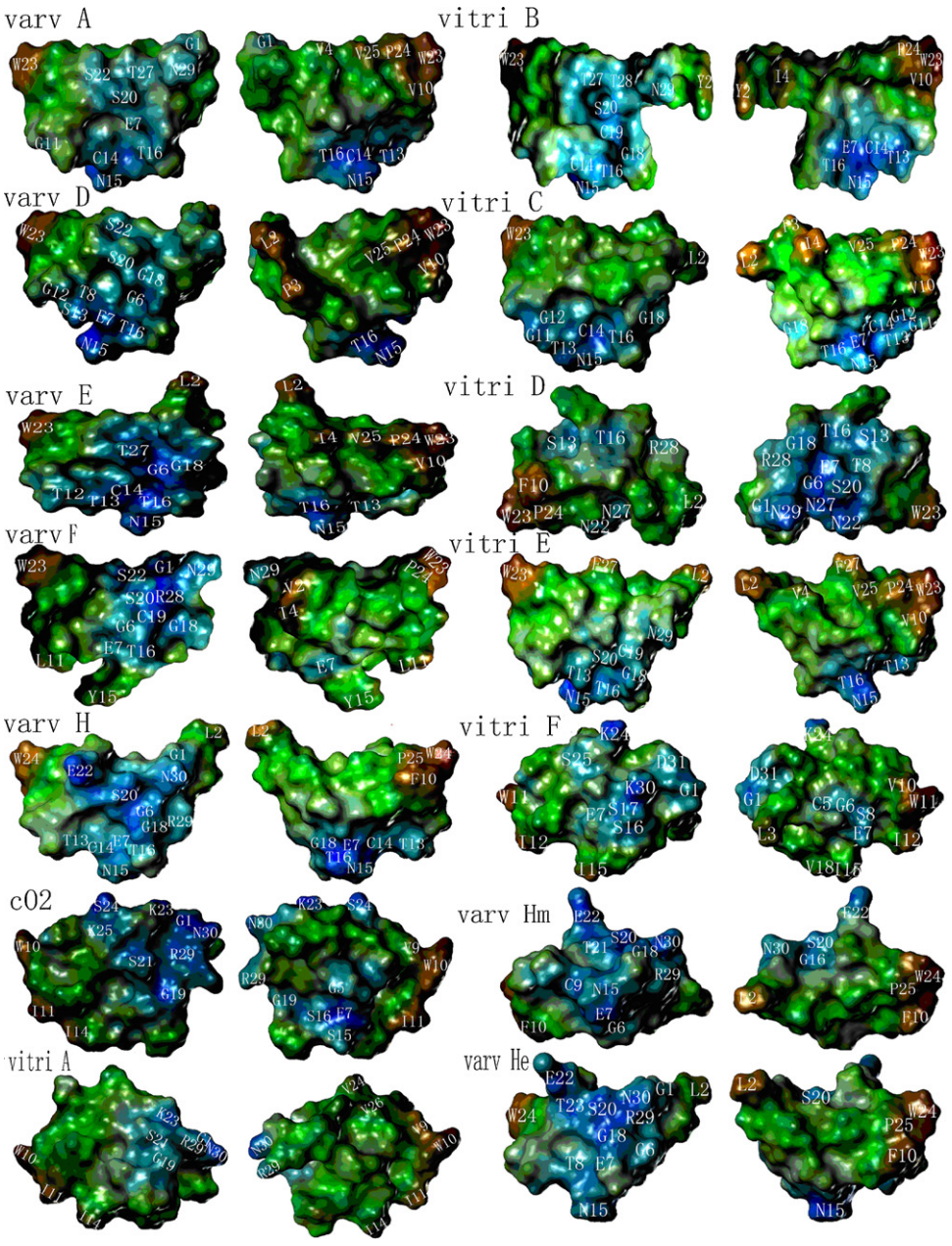

Fig. 4. Surface representations of cyclotides from *V. tricolor*. Highly hydrophobic areas are shaded brown, moderate hydrophobic areas are shaded green, and hydrophilic areas are shaded blue. Two views are shown for each molecule, rotated 180° from one another. Known cyclotides are shown on the left and novel cyclotides on the right. (For interpretation of the references to color in this figure legend, the reader is referred to the web version of the article.)

applied in previous studies. This new method is adaptable to a large amount of material and is convenient for laboratories without mass spectrometry or bio-assay facilities.

The experimentally derived sequences were compared with a database of cyclic proteins, CyBase, which currently contains >150 naturally occurring cyclotides and seven novel sequences were identified [50]. The novel cyclotide sequences from *V. tricolor* indicate that there are localized regions of conservation. The most conserved residues include the six Cys residues, the Glu in loop 1, and an Asn/Asp in loop 6. The six conserved Cys residues are required to form the landmark cystine knot of the cyclotides, which in combination with the cyclic backbone underpins their exceptional stability [5]. The Glu in loop 1 is also highly conserved across members of the cyclotide family, with only one known instance of its substitution (to an Asp) reported so far [36]. This Glu residue is believed to participate in a conserved hydrogen bond network that stabilizes the cyclotide fold [1,9,11,17,38]. More recently, the Glu has also been shown to be critical for cyclotide bioactivity, where modification of the Glu of two different cyclotides, either through methylation in cO2 or substitution to an Ala in kB1 [17,24,42], resulted in significant loss of activity compared to the unmodified parent cyclotide. The importance of this Glu in both structure and function is reinforced by its conservation in the new cyclotide sequences reported here. The Asn/Asp in loop 6 has been implicated in the biosynthetic pathway of the cyclotides and is situated at the C-terminal cyclization point of cyclotide precursor proteins [16,28,29,35,40].

Aside from these localized regions of conservation, cyclotide sequences show considerable variation, which is one reason why the cyclotide scaffold may be used to stabilize various linear epitopes through rational drug design [8,14]. Novel inter-cysteine loop sequences are present in vitri B–F, varv Hm and He, including loop 4

and loop 6 sequences, but in general the inter-cysteine loops in the new peptides reported here have been observed in cyclotides previously characterized, and are rearranged to form novel cyclotide sequences. Interestingly, we were able to isolate two sequences, which were similar to varv H but contained either a methylated or ethylated carboxyl group of Glu_{22}. Methylation or ethylation of the Glu side-chain, which probably occurred during the extraction procedure [30], means that Glu_{22} is uncharged at physiological conditions. It is not clear at this stage why the glutamic acid in loop 1 was not modified but further structural studies may provide clues to this answer.

A number of cyclotides have been reported to have hemolytic activity [27,46,49], and they are believed to interact with membranes *in vivo* [26,31,42,48]. In order to compare the membrane-disrupting activity of the cyclotides from *V. tricolor* with previously reported cyclotides [41,45], hemolytic assays were performed, and the results are shown in Fig. 3. The well known hemolytic peptide melittin was used as a positive control. Comparison of the novel cyclotides with those previously characterized from *V. tricolor*, reveals the cyclotides have varying levels of hemolytic activity, with vitri A showing the least hemolysis and vitri D being the most potent. Hydrophobicity of cyclotides has previously been shown to be important for hemolytic activity, as tricyclon A [35], a hybrid of the Möbius and the bracelet subfamilies, has the least hemolytic activity of all cyclotides tested up to now. However, the current study has shown that hydrophobicity is not the sole determinant of hemolytic activity, similar to the finding from alanine scanning mutagenesis of kB1 [42]. For instance, the least potent and most potent peptides in this study, vitri B and vitri D, respectively, are not the least hydrophobic or most hydrophobic, respectively. It is interesting to speculate that the lack of hemolytic activity of vitri B may be related to the lack of a basic residue in loop 6. Although mutational analysis is required to confirm the role of this charged residue, alanine scanning mutagenesis of kB1 [42] has shown that hemolytic activity is significantly decreased when the Arg residue in loop 6 is replaced with an alanine residue. Furthermore, cycloviolacin Y1 [49], another cyclotide with no basic amino acid residue in loop 6, has a low level of hemolytic activity. Given that kB1 and vitri B have 82% sequence identity it is likely that the substitution of the Arg for a Thr has a substantial influence on hemolytic activity. The basic amino acid residue in loop 6 is not only related to hemolytic activity, but also related to cytotoxic and nematocidal activity [25,44]. Interestingly this residue does not affect insecticidal activity [42]. Mutagenesis studies have not yet been done to follow up on the reported antimicrobial activity of cyclotides [46].

Various cyclotides have been shown to demonstrate cancer cell toxicity [23,24,32,44,45]. Therefore we tested the cyclotides from *V. tricolor* for cancer cell toxicity against five human cancer cell lines: U251, MDA-MB-231, A549, DU145, and BEL-7402. The clinically used natural product anti-cancer drug taxol was used as a positive control. Table 1 summarizes the results from these assays and reveals that several of the cyclotides from *V. tricolor* are active against cancer cells. Of the cyclotides tested in this study, the most potent cyclotides, which were vitri A, F, and cO2, are bracelet cyclotides and have similar IC_{50} values across the five cell lines tested. The values of the Möbius cyclotides vary from 37.18 to 74.39 μg/mL, about 10-fold higher than that of the bracelet cyclotides. Although the bracelet and the Möbius subfamilies have a similar ratio of hydrophobic amino acid residues in their sequences, the hydrophobic amino acid residues in the Möbius are more dispersed on the surfaces, compared to the bracelet subfamily. Therefore it may be that the placement of highly hydrophobic residues is important in determining the cytotoxicity of these cyclotides. Consistent with this suggestion, specific faces of cyclotides have previously been shown to interact with membranes [42]. Interestingly, varv Hm and varv He, which are methylated and ethylated derivatives of varv H, respectively, are less cytotoxic compared to varv H, suggesting that the surface charge of cyclotides is important for their activity. This finding is in agreement with a previous study showing that methylation of the carboxyl group of the Glu_6 in cO2 produced a 48-fold decrease in cytotoxicity [24].

For completeness we note that cyclotides are just one class of natural proteins that have been reported to have anti-cancer, anti-HIV or hemolytic activities. For example nebrodeolysin from the mushroom *Pleurotus nebrodensis* is a hemolytic protein with apoptosis-inducing and anti-HIV effects [33]. However, cyclotides are typically smaller than most natural proteins such as nebrodeolysin and their exceptional stability makes them particularly suitable as templates in drug design and agricultural applications [7,22].

In a summary, using improved isolation and detecting methods, we have shown that *V. tricolor* contains a suite of cyclotides, seven of which are new ones, *i.e.* vitri B–F, varv Hm, and He. Several cyclotides purified from *V. tricolor* exhibit potent cytotoxicity. Although hydrophobicity has previously been shown to correlate with hemolytic activity, the larger number of peptides tested in the current study suggests that overall hydrophobicity alone is not a predictor of hemolytic activity. The distribution of highly hydrophobic residues on the surface also appears to play a role in determining cytotoxicity. Overall, the trends in hemolytic and cytotoxic activity reported here have highlighted the complexity of the activity of cyclotides, which is most likely related to binding to membranes.

Acknowledgements

This work was supported by China/Australia Special Fund for S & T (NSFC and ARC), the National Natural Science Foundation of China (30725048), and National Basic Research Program of China (2009 CB522300), the Innovative Group Program from the Science and Technology Department of Yunnan Province (2008OC011) and the Fund of State Key Laboratory of Phytochemistry and Plant Resources in West China, Kunming Institute of Botany, Chinese Academy of Sciences. DJC is a National Health and Medical Research Council Professorial Fellow. NLD is Queensland Smart State Fellow.

Appendix A. Supplementary data

Supplementary data associated with this article can be found, in the online version, at doi:10.1016/j.peptides.2010.05.004.

References

[1] Barry DG, Daly NL, Bokesch HR, Gustafson KR, Craik DJ. Solution structure of the cyclotide palicourein: implications for the development of a pharmaceutical framework. Structure 2004;12:85–94.
[2] Brickmann J, Exner TE, Keil M, Marhöfer RJ. Molecular graphics—trends and perspectives. J Mol Model 2000;6:328–40.
[3] Carrascal N, Rizzo RC. Calculation of binding free energies for non-zinc chelating pyrimidine dicarboxamide inhibitors with MMP-13. Bioorg Med Chem Lett 2009;19:47–50.
[4] Claeson P, Goransson U, Johansson S, Luijendiik T, Bohlin L. Fractionation protocol for the isolation of polypeptides from plant biomass. J Nat Prod 1998;61:77–81.
[5] Colgrave ML, Craik DJ. Thermal, chemical, and enzymatic stability of the cyclotide kalata B1: the importance of the cyclic cystine Knot. Biochemistry 2004;43:5965–75.
[6] Colgrave ML, Kotze AC, Kopp S, McCarthy JS, Coleman GT, Craik DJ. Anthelmintic activity of cyclotides: in vitro studies with canine and human hookworms. Acta Trop 2009;109:163–6.
[7] Craik DJ. Circling the enemy: cyclic proteins in plant defence. Trends Plant Sci 2009;14:328–35.
[8] Craik DJ, Cemazar M, Daly NL. The cyclotides and related macrocyclic peptides as scaffolds in drug design. Curr Opin Drug Discov Develop 2006;9:251–60.
[9] Craik DJ, Daly NL. NMR as a tool for elucidating the structures of circular and knotted proteins. Mol Biosyst 2007;3:257–65.

[10] Craik DJ, Daly NL, Bond T, Waine C. Plant cyclotides: a unique family of cyclic and knotted proteins that defines the cyclic cystine knot structural motif. J Mol Biol 1999;294:1327–36.
[11] Craik DJ, Daly NL, Clark RJ, Jennings CV, Anderson M. Discovery and structure–function studies on the cyclotides: applications in drug design. J Pept Sci 2002;8:S68.
[12] Craik DJ, Daly NL, Mulvenna J, Plan MR, Trabi M. Discovery, structure and biological activities of the cyclotides. Curr Protein Pept Sci 2004;5:297–315.
[13] Craik DJ, Simonsen S, Daly NL. The cyclotides: novel macrocyclic peptides as scaffolds in drug design. Curr Opin Drug Discov Devel 2002;5:251–60.
[14] Daly NL, Rosengren KJ, Craik DJ. Discovery, structure and biological activities of cyclotides. Adv Drug Deliv Rev 2009;61:918–30.
[15] Fiser A, Do R, Sali A. Modeling of loops in protein structures. Protein Sci 2000;9:1753–73.
[16] Gillon AD, Saska I, Jennings CV, Guarino RF, Craik DJ, Anderson MA. Biosynthesis of circular proteins in plants. Plant J 2008;53:505–15.
[17] Goransson U, Herrmann A, Burman R, Haugaard-Jonsson LM, Rosengren KJ. The conserved Glu in the cyclotide cycloviolacin O2 has a key structural role. ChemBioChem 2009;10:2354–60.
[18] Goransson U, Luijendijk T, Johansson S, Bohlin L, Claeson P. Seven novel macrocyclic polypeptides from *Viola arvensis*. J Nat Prod 1999;62:283–6.
[19] Gustafson KR, Walton LK, Sowder RC, Johnson DG, Pannell LK, Cardellina JH, et al. New circulin macrocyclic polypeptides from *Chassalia parvifolia*. J Nat Prod 2000;63:176–8.
[20] Han HJ, Tan NH, Zeng GZ, Fan JT, Huang HQ, Ji CJR, et al. Natural inhibitors of DNA topoisomerase I with cytotoxicities. Chem Biodiver 2008;5:1364–8.
[21] Hansmann P, Kleinig H. Violaxanthin esters from *Viola tricolor* flowers. Phytochemistry 1982;21:238–9.
[22] Henriques ST, Craik DJ. Cyclotides as templates in drug design. Drug Discov Today 2010;15:57–64.
[23] Herrmann A, Burman R, Mylne JS, Karlsson G, Gullbo J, Craik DJ, et al. The alpine violet, *Viola biflora*, is a rich source of cyclotides with potent cytotoxicity. Phytochemistry 2008;69:939–52.
[24] Herrmann A, Svangard E, Claeson P, Gullbo J, Bohlin L, Goransson U. Key role of glutamic acid for the cytotoxic activity of the cyclotide cycloviolacin O2. Cell Mol Life Sci 2006;63:235–45.
[25] Huang YH, Colgrave ML, Clark RJ, Kotze AC, Craik DJ. Lysine-scanning mutagenesis reveals an amendable face of the cyclotide kalata B1 for the optimization of nematocidal activity. J Biol Chem 2010;285:10797–805.
[26] Huang YH, Colgrave ML, Daly NL, Keleshian A, Martinac B, Craik DJ. The biological activity of the prototypic cyclotide kalata B1 is modulated by the formation of multimeric pores. J Biol Chem 2009;284:20699–707.
[27] Ireland DC, Colgrave ML, Craik DJ. A novel suite of cyclotides from *Viola odorata*: sequence variation and the implications for structure, function and stability. Biochem J 2006;400:1–12.
[28] Ireland DC, Colgravel ML, Nguyencong P, Daly NL, Craik DJ. Discovery and characterization of a linear cyclotide from *Viola odorata*: implications for the processing of circular proteins. J Mol Biol 2006;357:1522–35.
[29] Jennings CV, West J, Waine C, Craik DJ, Anderson MA. Biosynthesis and insecticidal properties of plant cyclotides: the cyclic knotted proteins from *Oldenlandia affinis*. Proc Natl Acad Sci 2001;98:10614–9.
[30] Jung SY, Li Y, Wang Y, Chen Y, Zhao Y, Qin J. Complications in the assignment of 14 and 28 Da mass shift detected by mass spectrometry as *in vivo* methylation from endogenous proteins. Anal Chem 2008;80:1721–9.
[31] Kamimori H, Hall K, Craik DJ, Aguilar MI. Studies on the membrane interactions of the cyclotides kalata B1 and kalata B6 on model membrane systems by surface plasmon resonance. Anal Biochem 2005;337:149–53.
[32] Lindholm P, Goransson U, Johansson S, Claeson P, Gullbo J, Larsson R, et al. Cyclotides: a novel type of cytotoxic agents. Mol Cancer Ther 2002;1:365–9.
[33] Lv H, Kong Y, Yao Q, Zhang B, Leng F, Bian H, et al. Nebrodeolysin, a novel hemolytic protein from mushroom *Pleurotus nebrodensis* with apoptosis-inducing and anti-HIV-1 effects. Phytomedicine 2009;16:198–205.
[34] Molnar P, Szabolcs J, Radics L. Naturally occurring di-cis-violaxanthins from *Viola tricolor*: isolation and identification by ^{1}H NMR spectroscopy of four di-cis-isomers. Phytochemistry 1985;25:195–9.
[35] Mulvenna JR, Sando L, Craik DJ. Processing of a 22 kDa precursor protein to produce the circular protein tricyclon A. Structure 2005;13:691–701.
[36] Plan MR, Goransson U, Clark RJ, Daly NL, Colgrave ML, Craik DJ. The cyclotide fingerprint in *Oldenlandia affinis*: elucidation of chemically modified, linear and novel macrocyclic peptides. ChemBioChem 2007;8:1001–11.
[37] Plan MR, Saska I, Cagauan AG, Craik DJ. Backbone cyclised peptides from plants show molluscicidal activity against the rice pest *Pomacea canaliculata* (golden apple snail). J Agric Food Chem 2008;56:5237–41.
[38] Rosengren KJ, Daly NL, Plan MR, Waine C, Craik DJ. Twists, knots, and rings in proteins. Structural definition of the cyclotide framework. J Biol Chem 2003;278:8606–16.
[39] Saether O, Craik DJ, Campbell ID, Sletten K, Juul J, Norman DG. Elucidation of the primary and three-dimensional structure of the uterotonic polypeptide kalata B1. Biochemistry 1995;34:4147–58.
[40] Saska I, Gillon AD, Hatsugai N, Dietzgen RG, Hara-Nishimura I, Anderson MA, et al. An asparaginyl endopeptidase mediates in vivo protein backbone cyclization. J Biol Chem 2007;282:29721–8.
[41] Schoepke T, Hasan Agha MI, Kraft R, Otto A. Compounds with hemolytic activity from *Viola tricolor* L. and *Viola arvensis* Murray. Sci Pharm 1993;61:145–53.
[42] Simonsen SM, Sando L, Rosengren KJ, Wang CK, Colgrave ML, Daly NL, et al. Alanine scanning mutagenesis of the prototypic cyclotide reveals a cluster of residues essential for bioactivity. J Biol Chem 2008;283:9805–13.
[43] State Administration of Traditional Chinese Medicine of the People's Republic of China. Zhonghua Bencao. Shanghai: Shanghai Science and Technology Press; 1999. pp. 469–470.
[44] Svangard E, Burman R, Gunasekera S, Lovborg H, Gullbo J, Goransson U. Mechanism of action of cytotoxic cyclotides: cycloviolacin O2 disrupts lipid membranes. J Nat Prod 2007;70:643–7.
[45] Svangard E, Goransson U, Hocaoglu Z, Gullbo J, Larsson R, Claeson P, et al. Cytotoxic cyclotides from *Viola tricolor*. J Nat Prod 2004;67:144–7.
[46] Tam JP, Lu YA, Yang JL, Chiu KW. An unusual structural motif of antimicrobial peptides containing end-to-end macrocycle and cystine-knot disulfides. Proc Natl Acad Sci 1999;96:8913–8.
[47] Tan NH, Zhou J. Plant cyclopeptides. Chem Rev 2006;106:840–95.
[48] Wang CK, Colgrave ML, Ireland DC, Kaas Q, Craik DJ. Despite a conserved cystine knot motif, different cyclotides have different membrane binding modes. Biophys J 2009;97:1471–81.
[49] Wang CK, Colgrave ML, Gustafson KR, Ireland DC, Goransson U, Craik DJ. Anti-HIV cyclotides from the Chinese medicinal herb *Viola yedoensis*. J Nat Prod 2008;71:47–52.
[50] Wang CK, Kaas Q, Chiche L, Craik DJ. CyBase: a database of cyclic protein sequences and structures, with applications in protein discovery and engineering. Nucleic Acids Res 2008;36:D206–10.
[51] Witkowska-Banaszczak E, Bylka W, Matlawska I, Goslinska O, Muszynski Z. Antimicrobial activity of *Viola tricolor* herb. Fitoterapia 2005;76:458–61.
[52] Xu WY, Tang J, Ji CJ, He WJ, Tan NH. Application of a TLC chemical method to detection of cyclotides in plants. Chin Sci Bull 2008;53:1671–4.
[53] Zhang J, Liao B, Craik DJ, Li JT, Hu M, Shu WS. Identification of two suites of cyclotide precursor genes from metallophyte *Viola baoshanensis*: cDNA sequence variation, alternative RNA splicing and potential cyclotide diversity. Gene 2009;431:23–32.
[54] Zhou J, Tan NH. Application of a new TLC chemical method for detection of cyclopeptides in plants. Chin Sci Bull 2000;45:1825–32.